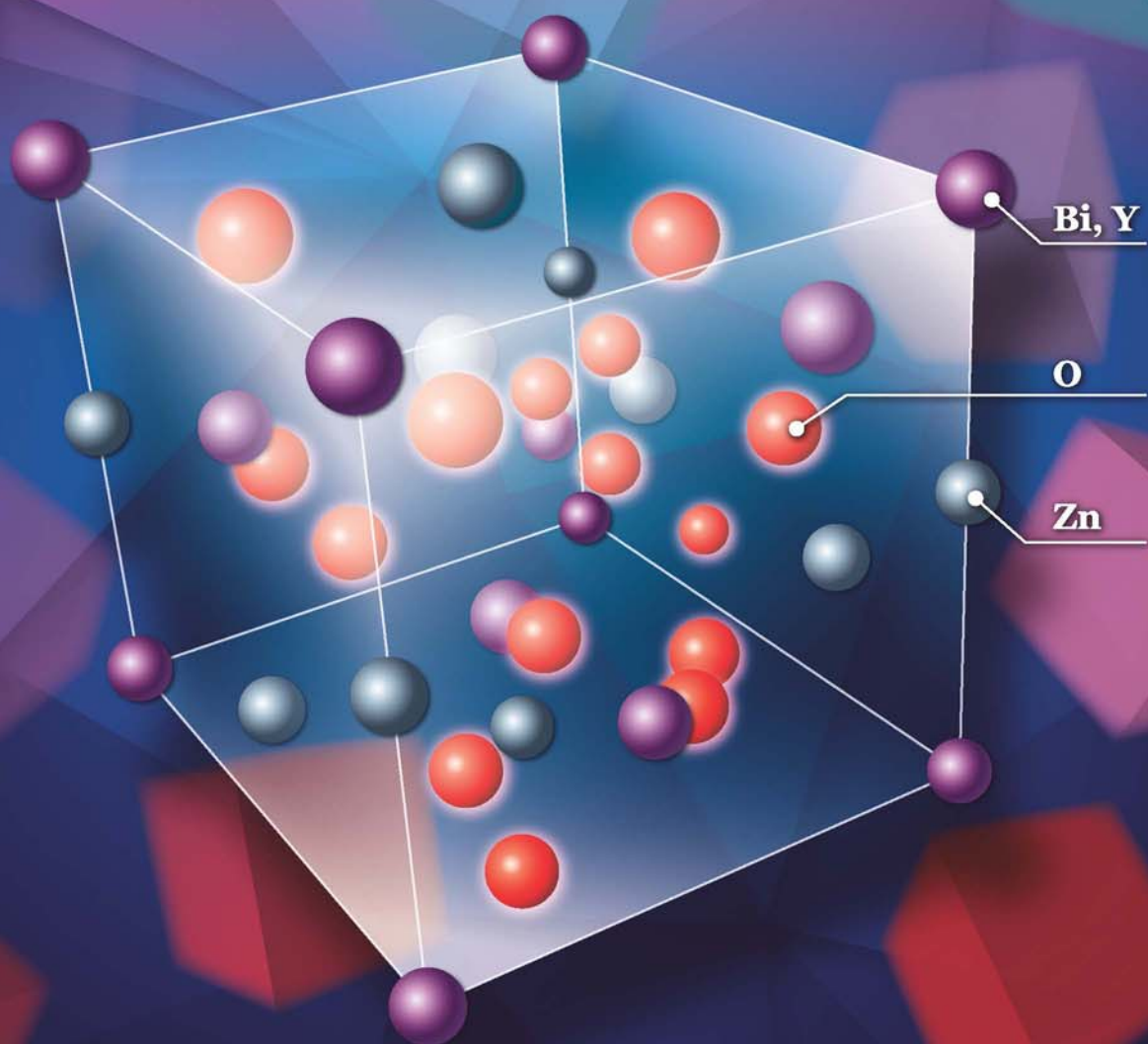


# JES

JOURNAL OF  
ENVIRONMENTAL  
SCIENCES

March 1, 2015 Volume 29  
www.jesc.ac.cn

ISSN 1001-0742  
CN 11-2629/X



Sponsored by  
Research Center for Eco-Environmental Sciences  
Chinese Academy of Sciences

- 1 A settling curve modeling method for quantitative description of the dispersion stability of carbon nanotubes in aquatic environments  
Lixia Zhou, Dunxue Zhu, Shujuan Zhang and Bingcai Pan
- 11 Antimony leaching release from brake pads: Effect of pH, temperature and organic acids  
Xingyun Hu, Mengchang He and Sisi Li
- 18 Molecular diversity of arbuscular mycorrhizal fungi at a large-scale antimony mining area in southern China  
Yuan Wei, Zhipeng Chen, Fengchang Wu, Hong Hou, Jining Li, Yuxian Shangguan, Juan Zhang, Fasheng Li and Qingru Zeng
- 27 Elevated CO<sub>2</sub> facilitates C and N accumulation in a rice paddy ecosystem  
Jia Guo, Mingqian Zhang, Xiaowen Wang and Weijian Zhang
- 34 Characterization of odorous charge and photochemical reactivity of VOC emissions from a full-scale food waste treatment plant in China  
Zhe Ni, Jianguo Liu, Mingying Song, Xiaowei Wang, Lianhai Ren and Xin Kong
- 45 Comparison between UV and VUV photolysis for the pre- and post-treatment of coking wastewater  
Rui Xing, Zhongyuan Zheng and Donghui Wen
- 51 Synthesis, crystal structure, photodegradation kinetics and photocatalytic activity of novel photocatalyst ZnBiYO<sub>4</sub>  
Yanbing Cui and Jingfei Luan
- 62 Sources and characteristics of fine particles over the Yellow Sea and Bohai Sea using online single particle aerosol mass spectrometer  
Huaiyu Fu, Mei Zheng, Caiqing Yan, Xiaoying Li, Huiwang Gao, Xiaohong Yao, Zhigang Guo and Yuanhang Zhang
- 71 Flower-, wire-, and sheet-like MnO<sub>2</sub>-deposited diatomites: Highly efficient absorbents for the removal of Cr(VI)  
Yucheng Du, Liping Wang, Jinshu Wang, Guangwei Zheng, Junshu Wu and Hongxing Dai
- 82 Methane and nitrous oxide emissions from a subtropical coastal embayment (Moreton Bay, Australia)  
Ronald S. Musenze, Ursula Werner, Alistair Grinham, James Udy and Zhiguo Yuan
- 97 Insights on the solubilization products after combined alkaline and ultrasonic pre-treatment of sewage sludge  
Xinbo Tian, Chong Wang, Antoine Prandota Trzcinski, Leonard Lin and Wun Jern Ng
- 106 Phosphorus recovery from biogas fermentation liquid by Ca-Mg loaded biochar  
Ci Fang, Tao Zhang, Ping Li, Rongfeng Jiang, Shubiao Wu, Haiyu Nie and Yingcai Wang
- 115 Characterization of the archaeal community fouling a membrane bioreactor  
Jinxue Luo, Jinsong Zhang, Xiaohui Tan, Diane McDougald, Guoqiang Zhuang, Anthony G. Fane, Staffan Kjelleberg, Yehuda Cohen and Scott A. Rice
- 124 Effect of six kinds of scale inhibitors on calcium carbonate precipitation in high salinity wastewater at high temperatures  
Xiaochen Li, Baoyu Gao, Qinyan Yue, Defang Ma, Hongyan Rong, Pin Zhao and Pengyou Teng
- 131 Experimental and molecular dynamic simulation study of perfluorooctane sulfonate adsorption on soil and sediment components  
Ruiming Zhang, Wei Yan and Chuanyong Jing
- 139 A fouling suppression system in submerged membrane bioreactors using dielectrophoretic forces  
Alaa H. Hawari, Fei Du, Michael Baune and Jorg Thöming

*(continued on inside back cover)*

## CONTENTS

- 146 A 1-dodecanethiol-based phase transfer protocol for the highly efficient extraction of noble metal ions from aqueous phase  
Dong Chen, Penglei Cui, Hongbin Cao and Jun Yang
- 151 Intracellular biosynthesis of Au and Ag nanoparticles using ethanolic extract of *Brassica oleracea* L. and studies on their physicochemical and biological properties  
Palaniselvam Kuppusamy, Solachuddin J.A. Ichwan, Narasimha Reddy Parine, Mashitah M. Yusoff, Gaanty Pragas Maniam and Natanamurugaraj Govindan
- 158 Forecasting of dissolved oxygen in the Guanting reservoir using an optimized NGBM (1,1) model  
Yan An, Zhihong Zou and Yanfei Zhao
- 165 Individual particle analysis of aerosols collected at Lhasa City in the Tibetan Plateau  
Bu Duo, Yunchen Zhang, Lingdong Kong, Hongbo Fu, Yunjie Hu, Jianmin Chen, Lin Li and A. Qiong
- 178 Design and demonstration of a next-generation air quality attainment assessment system for PM<sub>2.5</sub> and O<sub>3</sub>  
Hua Wang, Yun Zhu, Carey Jang, Che-Jen Lin, Shuxiao Wang, Joshua S. Fu, Jian Gao, Shuang Deng, Junping Xie, Dian Ding, Xuezheng Qiu and Shicheng Long
- 189 Soil microbial response to waste potassium silicate drilling fluid  
Linjun Yao, M. Anne Naeth and Allen Jobson
- 199 Enhanced catalytic complete oxidation of 1,2-dichloroethane over mesoporous transition metal-doped  $\gamma$ -Al<sub>2</sub>O<sub>3</sub>  
Abbas Khaleel and Muhammad Nawaz
- 210 Role of nitric oxide in the genotoxic response to chronic microcystin-LR exposure in human-hamster hybrid cells  
Xiaofei Wang, Pei Huang, Yun Liu, Hua Du, Xinan Wang, Meimei Wang, Yichen Wang, Tom K. Hei, Lijun Wu and An Xu

Available online at [www.sciencedirect.com](http://www.sciencedirect.com)

ScienceDirect

[www.journals.elsevier.com/journal-of-environmental-sciences](http://www.journals.elsevier.com/journal-of-environmental-sciences)JOURNAL OF  
ENVIRONMENTAL  
SCIENCES[www.jesc.ac.cn](http://www.jesc.ac.cn)

## Effect of six kinds of scale inhibitors on calcium carbonate precipitation in high salinity wastewater at high temperatures

Xiaochen Li, Baoyu Gao\*, Qinyan Yue, Defang Ma, Hongyan Rong, Pin Zhao, Pengyou Teng

Shandong Key Laboratory of Water Pollution Control and Resource Reuse, School of Environmental Science and Engineering, Shandong University, Shandong 250100, China

### ARTICLE INFO

#### Article history:

Received 14 April 2014

Revised 4 September 2014

Accepted 5 September 2014

Available online 7 January 2015

#### Keywords:

Scale inhibitor

Scale inhibition efficiency

High salinity

High temperature

Crystal growth

### ABSTRACT

Precipitation of calcium carbonate ( $\text{CaCO}_3$ ) scale on heat transfer surfaces is a serious and expensive problem widely occurring in numerous industrial processes. In this study, we compared the scale inhibition effect of six kinds of commercial scale inhibitors and screened out the best one (scale inhibitor SQ-1211) to investigate its scale inhibition performance in highly saline conditions at high temperature through static scale inhibition tests. The influences of scale inhibitor dosage, temperature, heating time and pH on the inhibition efficiency of the optimal scale inhibitor were investigated. The morphologies and crystal structures of the precipitates were characterized by Scanning Electron Microscopy and X-ray Diffraction analysis. Results showed that the scale inhibition efficiency of the optimal scale inhibitor decreased with the increase of the reaction temperature. When the concentration of  $\text{Ca}^{2+}$  was 1600 mg/L, the scale inhibition rate could reach 90.7% at 80°C at pH 8. The optimal scale inhibitor could effectively retard scaling at high temperature. In the presence of the optimal scale inhibitor, the main crystal structure of  $\text{CaCO}_3$  changed from calcite to aragonite.

© 2014 The Research Center for Eco-Environmental Sciences, Chinese Academy of Sciences.

Published by Elsevier B.V.

### Introduction

In recent years, more attention has been paid to the reuse of refinery wastewater in the petroleum industry after advanced treatment (Liu et al., 2011a, 2011b). Compared with natural water, there are a considerable number of inorganic ions and organic substrates in refinery wastewater, which would lead to easier scale formation in circulating cooling water systems (Liu et al., 2013). Scale formation on heat transfer surfaces is a severe problem widely occurring in numerous industrial processes including batch precipitation, power generation, water transport and oil or gas production (Demadis et al., 2007; El Dahan and Hegazy, 2000; Gu et al., 2012; Suharso et al., 2011). It will reduce the efficiency of heat transfer, increase energy consumption and cause unscheduled equipment shutdowns (Yang et al., 2001).

The most common and effective scale inhibition method is to use scale inhibitors. Scale inhibition derives from complex physical processes, such as adsorption, nucleation and crystal

growth processes, rather than chemical reactions (Ketrane et al., 2009). There is little understanding of the fundamental inhibition mechanisms, especially in quantitative aspects. Generally, researchers believe that the main mechanisms of scale inhibition include: (1) the threshold effect; (2) crystal distortion effect; (3) dispersion and (4) chelation (Darton, 2000; Lisitsin et al., 2005). Among them, threshold inhibition is the most appropriate method to control scale formation (Shakkthivel and Vasudevan, 2006). In other words, even a trace amount of inhibitor can prevent a scale layer from growing or adhering to a flow surface. Such low dosages are far less than the concentration of the scaling species, so chemical additives are also called “threshold inhibitors”.

In recent years, because of the strong chelation of their functional groups with metal ions and superior dispersion characteristic of macromolecules, copolymers have been regarded as satisfactory scale inhibitors and received much attention (Wang et al., 2009). A series of studies have proved that various

\* Corresponding author. E-mail: [baoyugao\\_sdu@aliyun.com](mailto:baoyugao_sdu@aliyun.com) (Baoyu Gao).



polyelectrolytes can retard crystal growth effectively (Al-Shammiri et al., 2000; Hasson et al., 1997, 1998; Smith, 1967). During crystal growth, different degrees of growth retardation for different crystal faces result in the formation of irregular crystals. The distortion of the crystal structure could increase the internal stress of crystals, which results in crystal fractures and prevents the deposition of microcrystals (Yang et al., 2001).

Polyphosphates, polyphosphonates and polycarboxylic acids are three popular copolymer scale inhibitors. Early research indicated that phosphate-containing additives had been adopted in over half of the drinking water treatment utilities in the United States (Casale, 2001). The phosphate-containing additives can sequester calcium and inhibit CaCO<sub>3</sub> scale precipitation even under the condition of calcite oversaturation (Marshall and Greaves, 1988). Polycarboxylic acids are another kind of copolymer scale inhibitor with cyclic or linear structure that can effectively inhibit CaCO<sub>3</sub> scale formation (Reddy and Hoch, 2001). The functional groups of polycarboxylic acids can chelate with Ca<sup>2+</sup> ions to inhibit the formation of CaCO<sub>3</sub> crystals and distort the crystal lattice to generate irregular crystals.

Though in recent decades many scientists have been studying scale inhibition, few have focused on scale inhibition in high salinity and oily wastewater at high temperature. In this research, we compared the inhibition effect of six kinds of commercial scale inhibitors and screened out the optimal one to investigate its scale inhibition performance on CaCO<sub>3</sub> scale using the static scale inhibition method. Compared with other scale inhibition methods, the static scale inhibition method is widely used because it requires simpler devices and shorter testing time than other methods. The influences of scale inhibitor dosage, reaction temperature, heating time and pH on scale inhibition efficiency of CaCO<sub>3</sub> precipitation were investigated. The morphology and crystal form of CaCO<sub>3</sub> scale were characterized by scanning electronic microscopy (SEM) and X-ray powder diffraction (XRD) analysis, respectively.

## 1. Experimental

### 1.1. Reagents and instruments

Potassium sulfate (K<sub>2</sub>SO<sub>4</sub>), magnesium chloride (MgCl<sub>2</sub>), ethylenediamine tetraacetic acid disodium salt (EDTA-2Na),

ethanol and triethanolamine were supplied by Tianjin Guangcheng Chemical Reagent Co., Ltd. (Tianjin, China). Calcium chloride anhydrous (CaCl<sub>2</sub>), sodium chloride (NaCl) and sodium bicarbonate (NaHCO<sub>3</sub>) were purchased from Tianjin Bodi Chemical Reagent Co., Ltd. (Tianjin, China). Eriochrome black T was obtained from Tianjin Damao Chemical Reagent Factory (Tianjin, China). Ammonium nitrate (NH<sub>4</sub>NO<sub>3</sub>) was purchased from Chengdu Kelong Chemical Reagent Factory (Chengdu, China). EDTA-magnesium disodium salt and ammonium chloride (NH<sub>4</sub>Cl) were supplied by Tianjin Kermel Chemical Reagent Co., Ltd. (Tianjin, China). Ammonium hydroxide (NH<sub>3</sub>·H<sub>2</sub>O) was purchased from Laiyang Kangde Chemical Reagent Co., Ltd. (Laiyang, China). The six scale inhibitors are: scale inhibitor SQ1211 (Shandong TianQing Science and Technology Development Co., Ltd., China); scale inhibitor 190, 265 (Nalco Company); and LinHai-4, LinHai-1 and LinHai-3 (Shandong LinHai Science and Technology Co., Ltd., China). All the reagents above are analytical reagent grade. Deionized water was used throughout the experiment.

### 1.2. Evaluation of the scale inhibition efficiency of inhibitors against CaCO<sub>3</sub> scale

In order to screen out the best scale inhibitor among six kinds of commercial scale inhibitors against CaCO<sub>3</sub> scale, a preliminary screening test was carried out. The experiment was performed according to the Chinese oil and gas industry standard evaluation method (SY/T 5673-1993). The oilfield wastewater in Shengli Oil Field (China) was used. The composition and analysis of the oilfield wastewater are shown in Table 1.

Experiments were carried out in 250 mL conical flasks heated at 80°C for 24 hr. First, a certain amount of oily wastewater was added into the flasks. Then six kinds of scale inhibitors were added into the wastewater, respectively. Next, the specimens were immersed in a thermostatic water bath at 80°C for 24 hr (the level of the water bath should be higher than that of the test solutions). When the solutions naturally cooled down to room temperature, they were filtered using medium-speed quantitative filter paper. The

**Table 1 – Compositions and analysis of the oilfield wastewater.**

Analyte	c(1/zB <sup>z-</sup> ) (mmol/L)	ρ(B) (mg/L)	Analyte	c(1/zB <sup>z-</sup> ) (mmol/L)	ρ(B) (mg/L)
Anion			Cation		
F <sup>-</sup>	0.000	0.00	Li <sup>+</sup>	0.000	0.00
Cl <sup>-</sup>	326.274	11566.42	Na <sup>+</sup>	239.990	5279.78
NO <sub>2</sub> <sup>-</sup>	0.000	0.00	NH <sub>4</sub> <sup>+</sup>	0.985	17.74
Br <sup>-</sup>	0.000	0.00	K <sup>+</sup>	1.932	75.54
NO <sub>3</sub> <sup>-</sup>	1.197	74.21	Mg <sup>2+</sup>	7.312	88.84
SO <sub>4</sub> <sup>2-</sup>	5.028	241.35	Ca <sup>2+</sup>	80.109	1605.39
OH <sup>-</sup>	0.000	0.00	Sr <sup>2+</sup>	0.000	0.00
CO <sub>3</sub> <sup>2-</sup>	0.000	0.00	Ba <sup>2+</sup>	0.000	0.00
HCO <sub>3</sub> <sup>-</sup>	1.377	84.02			
Amount	333.876	11966.00	Amount	330.328	7067.29
pH		6.5			
Degree of mineralization		19033.29	Permanent hardness		4306.51
ρ(ΣB) (mg/L)			ρ(CaCO <sub>3</sub> ) (mg/L)		
Total hardness		4375.43	Temporary hardness		140.13
ρ(CaCO <sub>3</sub> ) (mg/L)			ρ(CaCO <sub>3</sub> ) (mg/L)		
Total alkalinity		68.92	Negative hardness		0.00
ρ(CaCO <sub>3</sub> ) (mg/L)			ρ(CaCO <sub>3</sub> ) (mg/L)		

$\text{Ca}^{2+}$  concentrations in test and blank solutions were titrated by an EDTA standard solution. The scale inhibition efficiency was calculated as follows:

$$\eta = \frac{\rho_2 - \rho_0}{\rho_1 - \rho_0} \times 100\% \quad (1)$$

where,  $\rho_0$  (mg/L) is the mass concentration of  $\text{Ca}^{2+}$  in the absence of scale inhibitor in the blank solution after the test.  $\rho_2$  (mg/L) is the mass concentration of  $\text{Ca}^{2+}$  in the presence of scale inhibitor in the test solution after the test.  $\rho_1$  (mg/L) is the mass concentration of  $\text{Ca}^{2+}$  before the test.

As a result, the scale inhibitor SQ1211 showed the best scale inhibition effect compared with other inhibitors (Section 2.1) and was used in following experiments.

### 1.3. Inhibition performance of the optimal scale inhibitor against $\text{CaCO}_3$ scale

After the preliminary screening test, the optimal scale inhibitor was used for further study. The scale inhibition efficiency of the optimal scale inhibitor was also determined according to the Chinese oil and gas industry standard evaluation method (SY/T 5673-1993). The composition of the sample solution used in these experiments was based on that of the oilfield wastewater in Shengli Oil Field (China). The exact experimental procedure was described in Section 1.2. The detailed process of preparing the water sample solution was as follows. First, 35 mL of deionized water was added into a 250 mL conical flask. Then, 25 mL of  $\text{CaCl}_2$  solution (0.2 mol/L), 50 mL of NaCl solution (0.6 mol/L), 1.25 mL of  $\text{NH}_4\text{NO}_3$  solution (0.1 mol/L) and 5 mL of  $\text{MgCl}_2$  solution (0.1 mol/L) were added into the conical flask in sequence. In order to investigate the effect of scale inhibitor SQ-1211 on the scale inhibition performance, a SQ1211 sample was added into the above sample solution at 1 g/L and shaken to ensure complete mixing. Then, 5 mL of  $\text{NH}_4\text{Cl}-\text{NH}_3\cdot\text{H}_2\text{O}$  buffer solution with pH = 10 was added. Finally, 1.25 mL of  $\text{NaHCO}_3$  solution (0.1 mol/L) and 2.5 mL of  $\text{K}_2\text{SO}_4$  (0.1 mol/L) was slowly added (shaking while adding).

### 1.4. Sample collection of $\text{CaCO}_3$ scale

25 mL of  $\text{CaCl}_2$  solution (0.2 mol/L) was added into a 250 mL conical flask. Then 50 mL of NaCl solution (0.6 mol/L) was added. Next, a scale inhibitor solution sample was added at 1 g/L. Finally, 50 mL of  $\text{NaHCO}_3$  solution (0.2 mol/L) was slowly poured into the above mixture. Then the blank and test sample were immersed into a thermostatic water bath at 80°C for 10 hr. After that, the samples were dried to collect the  $\text{CaCO}_3$  scale for further analysis.

### 1.5. Characterization of $\text{CaCO}_3$ crystal

The sample of  $\text{CaCO}_3$  scale obtained according to Section 1.4 was characterized by SEM and XRD analyses. Micrographs of  $\text{CaCO}_3$  crystal were taken using a HITACHI S-520 scanning electron microscope (Hitachi Limited, Japan). The samples were pretreated by gold sputtering before imaging. XRD experiments were carried out on a Rigaku D/MAX-rA XRD diffractometer (Rigaku Corporation, Japan) with Cu  $K\alpha$  radiation at  $\lambda = 1.54184 \text{ \AA}$ .

## 2. Results and discussion

### 2.1. Preliminary screening test of scale inhibitors

The scale inhibition efficiencies of six kinds of scale inhibitors at different dosages are shown in Fig. 1. When the dosage of SQ1211 was 11 mg/L, the scale inhibition efficiency was as high as 91%, but the scale inhibition efficiency decreased to 57% when the dosage was 20 mg/L. When the dosage was more than 20 mg/L, the scale inhibition efficiency of SQ1211 increased slightly from 20 to 30 mg/L and then decreased with the increase of dosage. When the dosage increased from 10 to 50 mg/L, the scale inhibition efficiency of scale inhibitor 190 and 265 had first increasing and then decreasing trends with the increase of dosage, while scale inhibitor LinHai-4, LinHai-1 and LinHai-3 decreased with the increase of dosage and stabilized finally.

As illustrated in Fig. 1, SQ1211, which consisted of polycarboxylic acids and an organic phosphine-carboxylic acid copolymer, had the best scale inhibition effect compared with other inhibitors, and the highest scale inhibition efficiency could reach 91%.

### 2.2. Inhibition performance of the optimal scale inhibitor against $\text{CaCO}_3$ scale

#### 2.2.1. Effect of dosage and temperature on inhibition efficiency

The effect of scale inhibitor dosage on scale inhibition efficiency was investigated and the results are shown in Fig. 2. A simulated wastewater of high salinity was prepared according to Table 1. The heating time was 10 hr; concentration of  $\text{CaCl}_2$  and  $\text{NaHCO}_3$  were 0.04 mol/L and 0.001 mol/L, respectively. It can be seen from Fig. 2 that the scale inhibition efficiency rose with the increase of the scale inhibitor dosage when the dosage was below 11 mg/L. The reason was that a smaller amount of active scale inhibitor contributed to the adsorption of  $\text{CaCO}_3$  and blocked its formation at low scale inhibitor dosages, thereby  $\text{CaCO}_3$  precipitated more easily. When the scale inhibitor dosage reached 11 mg/L, it had the highest efficiency. After the dosage of the scale inhibitor exceeded the optimal

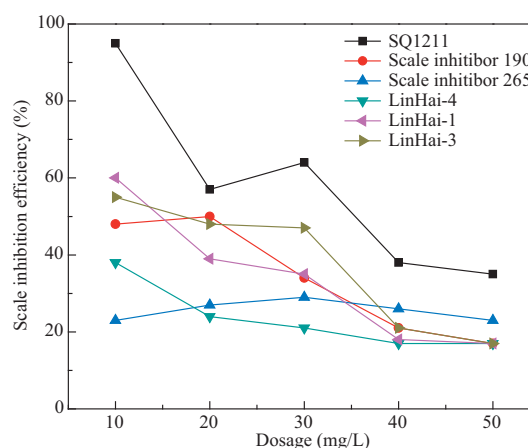
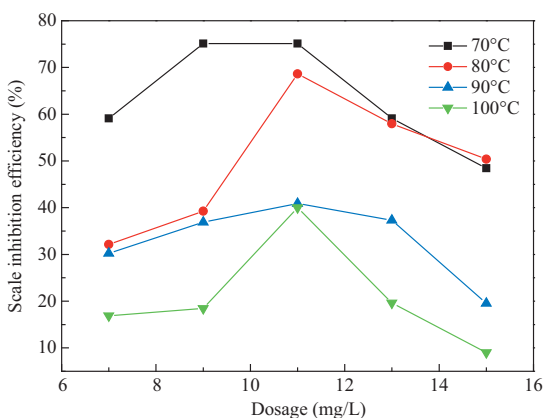


Fig. 1 – Scale inhibition efficiencies of six kinds of scale inhibitors at different dosages at 80°C for 24 hr.



**Fig. 2 – Effects of dosage and temperature on scale inhibition efficiency for 10 hr.**

concentration, the scale inhibition efficiency declined as the dosage increased. This phenomenon could be explained by the threshold effect, which indicated that the dosage exceeded the optimal concentration, so that the scale inhibition efficiency did not increase when the scale inhibitor dosage increased.

It can also be observed that the scale inhibition efficiency was significantly affected by the reaction temperature. The scale inhibition efficiency declined with the increase of temperature. The highest scale inhibition efficiency could reach 75.1% and 69% when the temperature was 70 and 80°C, respectively. Moreover, the result showed that when the temperature was over 80°C, the scale inhibition efficiency had an obvious reduction at the optimal concentration. The highest scale inhibition efficiency at 90°C was only 40.9%, which was a little higher than that at 100°C. It is well known that the solubility of  $\text{CaCO}_3$  decreases with increasing temperature. In addition, the scale layer formed more rapidly and became thicker as temperature increased, which could also reduce the scale inhibition efficiency. So the scale inhibition efficiency decreased as temperature rose from 70 to 100°C.

#### 2.2.2. Effect of heating time on concentration of $\text{Ca}^{2+}$

According to the result obtained from Section 2.2.1, the influence of heating time on concentration of  $\text{Ca}^{2+}$  was investigated at 80°C, and the concentration of SQ1211 was 11 mg/L. The initial concentration of  $\text{Ca}^{2+}$  was 1650 mg/L. As observed in Fig. 3, the concentration of  $\text{Ca}^{2+}$  in solution decreased with the increase of heating time with and without scale inhibitor. The difference is that in the presence of scale inhibitor, the concentration of  $\text{Ca}^{2+}$  was much higher than that in the blank sample without scale inhibitor. In other words, the scale inhibitor can significantly retard the scaling tendency. The concentration of  $\text{Ca}^{2+}$  showed a significant declining trend from 1650 to 1568 mg/L during the first 5 hr in the absence of scale inhibitor, while the concentration of  $\text{Ca}^{2+}$  in the sample only decreased from 1650 to 1622 mg/L when scale inhibitor was used. As heating time went up, it could be clearly observed that the scale inhibitor had a significant effect on slowing down the formation of scaling. The reason may be that the scale inhibitor not only chelated with  $\text{Ca}^{2+}$  in the solution but also occupied the active growth sites of the

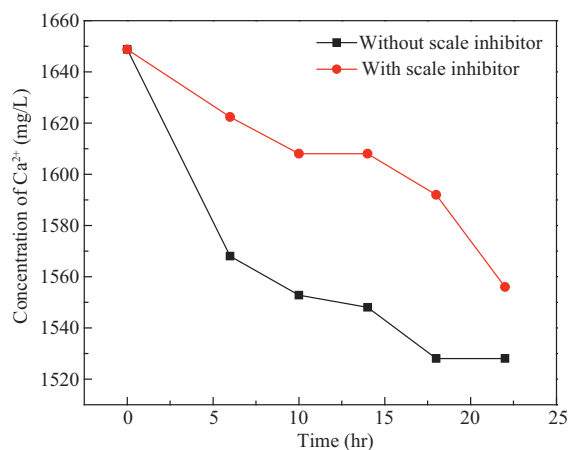


**Fig. 3 – Effects of heating time on the concentration of  $\text{Ca}^{2+}$  at 80°C.**

crystal surface, which led to lattice distortion. After 18 hr, the concentration of  $\text{Ca}^{2+}$  in the sample with scale inhibitor declined greatly. This might be caused by the destabilization of the scale inhibitor. However, the concentration of  $\text{Ca}^{2+}$  in the blank solution began to stabilize, because there was insufficient  $\text{CO}_3^{2-}$  in the solution to form a precipitate. In conclusion, the scale inhibitor had a good effect on retarding the formation of  $\text{CaCO}_3$  scale.

#### 2.2.3. Effect of pH on inhibition efficiency

The influence of pH on scale inhibition efficiency was investigated at 80°C with a heating period of 10 hr, and the concentration of the scale inhibitor SQ1211 was 11 mg/L. It can be seen from Fig. 4 that the scale inhibition efficiency increased at first and then decreased with the increase of pH from 6 to 10. The scale inhibitor had the highest efficiency of 90.7% at pH 8. Compared with alkaline conditions, the scale inhibition efficiency was lower under acid conditions, maybe because the scale inhibitor was less stable under acid conditions. In addition, the concentration of  $\text{Ca}^{2+}$  decreased with the increase of pH without scale inhibitor, while the concentration

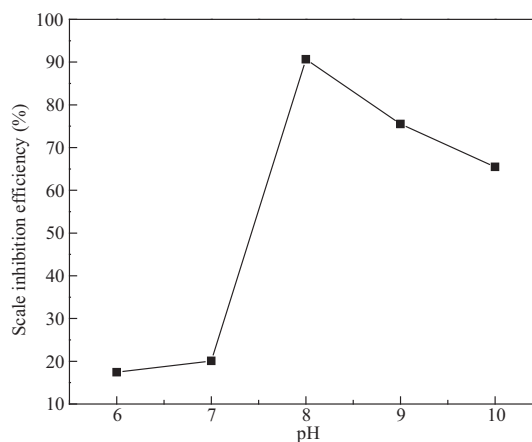


**Fig. 4 – Effects of pH on scale inhibition efficiency at 80°C for 10 hr.**

of  $\text{Ca}^{2+}$  remained at a high level at different pH in the presence of scale inhibitor. Hence the scale inhibition efficiency was better under alkaline conditions. With the increase of pH, the concentration of  $\text{OH}^-$  increased and the reaction equilibrium between  $\text{OH}^-$  and  $\text{HCO}_3^-$  shifted to the right, which led to the decrease of  $\text{HCO}_3^-$  and the increase of  $\text{CO}_3^{2-}$ . As a consequence, the  $\text{CaCO}_3$  precipitated more easily and the scale inhibition efficiency decreased. In addition, the carboxylic acid group ( $-\text{COOH}$ ) was unstable in alkaline conditions, because the ionization degree of the carboxylic acid group increased under this condition, and only  $\text{C}=\text{O}$  from the completely protonated scale inhibitor with  $-\text{COOH}$  groups could form hydrogen bonds with the water molecules from the surface of insoluble salt nuclei. Hence the scale inhibition efficiency decreased as pH increased from 8 to 10.

#### 2.2.4. SEM micrographs of $\text{CaCO}_3$ crystals in the absence and presence of scale inhibitor

In order to investigate the effect of the scale inhibitor on the growth and morphology changes of  $\text{CaCO}_3$  crystals, the  $\text{CaCO}_3$  scales formed in the absence and presence of the optimal scale inhibitor were characterized by SEM analysis. The scanning micrographs of  $\text{CaCO}_3$  crystals are shown in Fig. 5. As shown in Fig. 5a, the  $\text{CaCO}_3$  crystals in the blank sample had regular shape with clear rhombohedral structure. They also had a glossy surface and compact structure. This indicated that the  $\text{CaCO}_3$  crystals in the blank sample without scale inhibitor were mainly composed of calcite, which was the most thermodynamically stable form of  $\text{CaCO}_3$  crystal (Xyla et al., 1992). When the scale inhibitor was added into the sample, the  $\text{CaCO}_3$  crystals changed obviously from regular cube shapes and glossy surfaces with compact structure to flower and rod structures and rough surfaces with relatively loose accumulation (Fig. 5b). It is well known that calcite, aragonite and vaterite have rhomboidal, needle/rod and spherical structures, respectively (Gopi and Subramanian, 2012). So we could conclude that the main crystal structure of  $\text{CaCO}_3$  had changed from calcite to aragonite after adding the scale inhibitor.

The major components of the optimal scale inhibitor were polycarboxylic acids and organic phosphine-carboxylic acid copolymer. During  $\text{CaCO}_3$  crystal growth, the  $-\text{P}(\text{O})(\text{OH})_2$  group could affect the scale inhibition efficiency by occupying the active sites on the surface of  $\text{CaCO}_3$  crystals and changing the

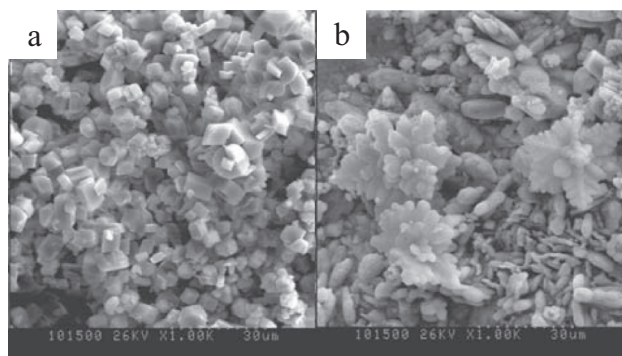


**Fig. 5 – Scanning Electron Microscope (SEM) micrographs of the  $\text{CaCO}_3$  precipitation in the absence of scale inhibitor (a), in the presence of scale inhibitor (b).**

extent of chemical bonding with the surface (Sondi and Matijević, 2001). In addition, the  $-\text{P}(\text{O})(\text{OH})_2$  group and  $-\text{COO}^-$  group had a high chelating ability toward calcium ions to form stable chelation compounds (Demadis and Katarachia, 2004; Gal et al., 1996; Hasson et al., 1997). These would interfere with the nucleation and growth of  $\text{CaCO}_3$  crystals so that the crystals became irregular (Qiang et al., 2013). The distortion in the  $\text{CaCO}_3$  crystals increased their internal stress, which would lead to crystal fractures and inhibition of deposition of microcrystals. Previous studies suggested that aragonite and vaterite could be more thermodynamically stable than calcite at certain temperatures or in the presence of some inhibitors (Kralj et al., 1997). Thus it was illustrated that the aragonite and vaterite possessed higher thermodynamic stability than calcite in the presence of the scale inhibitor SQ1211. Because aragonite and vaterite have a higher solubility product and free energy than calcite (Knez and Pohar, 2005), the scale was easy to dissolve and can be washed away by water. Consequently, the  $\text{CaCO}_3$  crystals deposited in the experimental process had difficulty adhering to the surface of the beaker and scale inhibition was obtained.

#### 2.2.5. XRD analysis of $\text{CaCO}_3$ crystals in the absence and presence of the optimal scale inhibitor

The  $\text{CaCO}_3$  crystals were also characterized by XRD analysis. Fig. 6 presents the XRD images of  $\text{CaCO}_3$  crystals in the absence and presence of the scale inhibitor. The XRD patterns in Fig. 6a show that calcite was the main crystal form in  $\text{CaCO}_3$  precipitation without scale inhibitor. The diffraction peak strength of the calcite crystal deposited in the blank sample without scale inhibitor was strongest at  $29.242^\circ$  (the characteristic crystal face 104 of the calcite), which confirmed that the 104 face was the major growth surface without scale inhibitor. In addition, the diffraction peaks at  $39.223^\circ$ ,  $43.057^\circ$  and  $48.378^\circ$  corresponded to the calcite crystal faces 113, 202 and 118, respectively. This indicated that calcite was the dominant crystal form in the absence of scale inhibitor. This result was consistent with the conclusion drawn from Fig. 5a. Yet, after adding the scale inhibitor, the characteristic diffraction peaks of calcite observed in Fig. 6a were simultaneously invisible in Fig. 6b, which illustrated that the growth of the crystal faces 104, 113, 202 and 118 was completely inhibited by the scale inhibitor. Instead, the diffraction peak at  $31.602^\circ$  (the characteristic crystal face 006 of calcite) was observed and it had the strongest diffraction peak strength, which illustrated that the face 006 became the major growth surface in the presence of scale inhibitor. In addition, the diffraction peaks of aragonite phase at  $45.342^\circ$ ,  $56.313^\circ$  and  $66.261^\circ$  are also visible in Fig. 6b, which correspond to the 221, 042 and 312 crystal faces. This indicated that the scale inhibitor could not only greatly inhibit the crystal growth of calcite but also transform a large amount of calcite phase to the aragonite phase. In other words, the aragonite phase was stabilized kinetically in the presence of the scale inhibitor. A previous study has shown that vaterite was the initial phase formed in  $\text{CaCO}_3$  supersaturated solution, and it could be transformed to calcite in the absence of scale inhibitor (Chakraborty et al., 1994), which was also confirmed by this study. In the presence of scale inhibitor, most of the vaterite phase was transformed to mixtures of the calcite phase and aragonite phase. It is known that calcite is the most



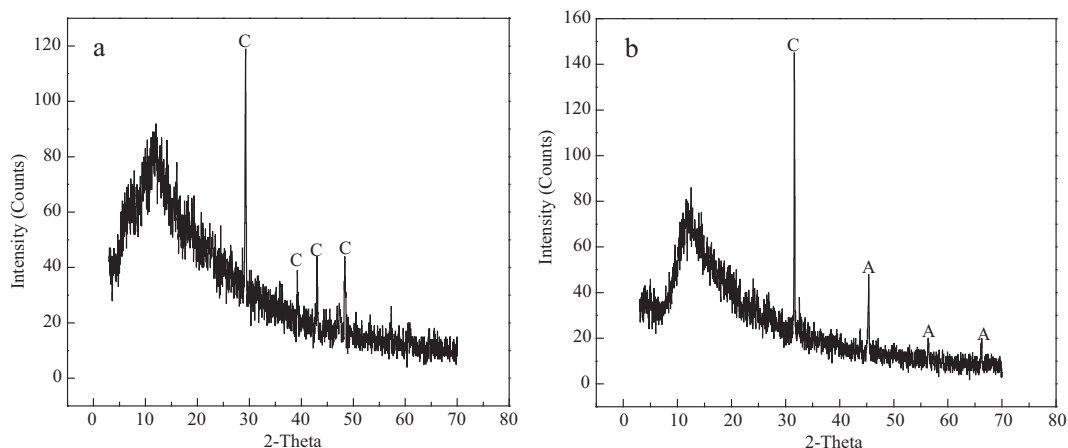


**Fig. 6 – XRD images of the  $\text{CaCO}_3$  precipitate in the absence of scale inhibitor (a), in the presence of scale inhibitor (b). A: aragonite; C: calcite.**

thermodynamically stable form of  $\text{CaCO}_3$ , so the formed scale was easy to attach on the surface of the heat exchanger and hard to wash away. However, the scale inhibitor changed the crystal growth habit and destroyed the crystal structure. Compared with calcite, aragonite had loose accumulation and higher solubility product and free energy, which meant that the highly dispersed and unstable crystal was easy to dissolve and can be washed away by water. In conclusion, the loss of heat transfer can be minimized and scale inhibition can be obtained.

### 3. Conclusion

(1) Of the six kinds of scale inhibitors, the scale inhibitor SQ1211 had the best scale inhibition effect at high temperatures. In the scale inhibition system, the inhibition efficiency was influenced by scale inhibitor dosage, reaction temperature, heating time and pH. (2) The optimal dosage of SQ1211 was 11 mg/L when the concentration of  $\text{Ca}^{2+}$  was as high as 1600 mg/L. Moreover, SQ1211 can significantly retard the scaling tendency. (3) The scale inhibition efficiency decreased as the reaction temperature (ranging from 70 to 100°C) increased. The scale inhibition efficiency could reach 75.1% at 70°C. (4) Initially, the scale inhibition efficiency increased gradually in the pH range 6–8, and then decreased with pH further increasing. At constant temperature of 80°C, the highest inhibition efficiency was 90.7% at pH 8. (5) In the presence of SQ1211, the highly dispersed and unstable aragonite phase became the main crystal form in  $\text{CaCO}_3$  scale, which would cause the scale to dissolve and be washed away by water easily. (6) The reason why the scale inhibition effect of SQ1211 in the oilfield wastewater was higher than in the simulated wastewater still needs further study.

### Acknowledgments

This research was supported by the Major Bidding Projects in Shandong Province (No. SDZS-2012-SHBT01). The kind suggestions from the anonymous reviewers are greatly appreciated.

### REFERENCES

- Al-Shammiri, M., Safar, M., Al-Dawas, M., 2000. Evaluation of two different antiscalants in real operation at the Doha research plant. *Desalination* 128 (1), 1–16.
- Casale, R.J., 2001. Improving chemical handling procedures can help reduce associated treatment problems. *J. Am. Water Works Assoc.* 93 (9), 95–106.
- Chakraborty, D., Agarwal, V., Bhatia, S., Bellare, J., 1994. Steady-state transitions and polymorph transformations in continuous precipitation of calcium carbonate. *Ind. Eng. Chem. Res.* 33 (9), 2187–2197.
- Darton, E.G., 2000. Membrane chemical research: centuries apart. *Desalination* 132 (1–3), 121–131.
- Demadis, K.D., Katarachia, S.D., 2004. Metal-phosphonate chemistry: synthesis, crystal structure of calcium-aminotris-(methylene phosphonate) and inhibition of  $\text{CaCO}_3$  crystal growth. *Phosphorus Sulfur* 179 (3), 627–648.
- Demadis, K.D., Mavredaki, E., Stathoulopoulou, A., Neofotistou, E., Mantzaridis, C., 2007. Industrial water systems: problems, challenges and solutions for the process industries. *Desalination* 213 (1–3), 38–46.
- El Dahan, H.A., Hegazy, H.S., 2000. Gypsum scale control by phosphate ester. *Desalination* 127 (2), 111–118.
- Gal, J.-Y., Bollinger, J.-C., Tolosa, H., Gache, N., 1996. Calcium carbonate solubility: a reappraisal of scale formation and inhibition. *Talanta* 43 (9), 1497–1509.
- Gopi, S.P., Subramanian, V.K., 2012. Polymorphism in  $\text{CaCO}_3$ —Effect of temperature under the influence of EDTA (disodium salt). *Desalination* 297, 38–47.
- Gu, X., Qiu, F., Zhou, X., Qi, J., Zhou, Y., Guo, X., et al., 2012. Preparation, characterization, and inhibition efficiency of quadripolymer for use as scale inhibitor. *Int. J. Polym. Anal. Charact.* 17 (5), 321–332.
- Hasson, D., Bramson, D., Limoni-Relis, B., Semiat, R., 1997. Influence of the flow system on the inhibitory action of  $\text{CaCO}_3$  scale prevention additives. *Desalination* 108 (1), 67–79.
- Hasson, D., Semiat, R., Bramson, D., Busch, M., Limoni-Relis, B., 1998. Suppression of  $\text{CaCO}_3$  scale deposition by anti-scalants. *Desalination* 118 (1–3), 285–296.
- Ketrane, R., Saidani, B., Gil, O., Leleyter, L., Baraud, F., 2009. Efficiency of five scale inhibitors on calcium carbonate precipitation from hard water: effect of temperature and concentration. *Desalination* 249 (3), 1397–1404.

- Knez, S., Pohar, C., 2005. The magnetic field influence on the polymorph composition of  $\text{CaCO}_3$  precipitated from carbonized aqueous solutions. *J. Colloid Interface Sci.* 281 (2), 377–388.
- Kralj, D., Brečević, L., Kontrec, J., 1997. Vaterite growth and dissolution in aqueous solution III. Kinetics of transformation. *J. Cryst. Growth* 177 (3), 248–257.
- Lisitsin, D., Yang, Q., Hasson, D., Semiat, R., 2005. Inhibition of  $\text{CaCO}_3$  scaling on RO membranes by trace amounts of zinc ions. *Desalination* 183 (1–3), 289–300.
- Liu, F., Zhao, C.C., Xia, L., Yang, F., Chang, X., Wang, Y.Q., 2011a. Biofouling characteristics and identification of preponderant bacteria at different nutrient levels in batch tests of a recirculating cooling water system. *Environ. Technol.* 32 (8), 901–910.
- Liu, F., Chang, X., Yang, F., Wang, Y., Wang, F., Dong, W., et al., 2011b. Effect of oxidizing and non-oxidizing biocides on biofilm at different substrate levels in the model recirculating cooling water system. *World J. Microbiol. Biotechnol.* 27 (12), 2989–2997.
- Liu, F., Lu, X., Yang, W., Lu, J., Zhong, H., Chang, X., et al., 2013. Optimizations of inhibitors compounding and applied conditions in simulated circulating cooling water system. *Desalination* 313, 18–27.
- Marshall, A., Greaves, B., 1988. A new total organic approach for the control of corrosion and deposition in cooling water systems. 4th Middle East Corrosion Conference. I, Bahrain.
- Qiang, X., Sheng, Z., Zhang, H., 2013. Study on scale inhibition performances and interaction mechanism of modified collagen. *Desalination* 309, 237–242.
- Reddy, M.M., Hoch, A.R., 2001. Calcite crystal growth rate inhibition by polycarboxylic acids. *J. Colloid Interface Sci.* 235 (2), 365–370.
- Shakkthivel, P., Vasudevan, T., 2006. Acrylic acid-diphenylamine sulphonic acid copolymer threshold inhibitor for sulphate and carbonate scales in cooling water systems. *Desalination* 197 (1–3), 179–189.
- Smith, B.R., 1967. Scale prevention by addition of polyelectrolytes. *Desalination* 3 (3), 263–268.
- Sondi, I., Matijević, E., 2001. Homogeneous precipitation of calcium carbonates by enzyme catalyzed reaction. *J. Colloid Interface Sci.* 238 (1), 208–214.
- Suharso, Buhani, Bahri, S., Endaryanto, T., 2011. Gambier extracts as an inhibitor of calcium carbonate ( $\text{CaCO}_3$ ) scale formation. *Desalination* 265 (1–3), 102–106.
- Wang, C., Li, S.-p, Li, T.-d., 2009. Calcium carbonate inhibition by a phosphonate-terminated poly(maleic-co-sulfonate) polymeric inhibitor. *Desalination*. 249 (1), 1–4.
- Xyla, A.G., Mikroyannidis, J., Koutsoukos, P.G., 1992. The inhibition of calcium carbonate precipitation in aqueous media by organophosphorus compounds. *J. Colloid Interface Sci.* 153 (2), 537–551.
- Yang, Q., Liu, Y., Gu, A., Ding, J., Shen, Z., 2001. Investigation of calcium carbonate scaling inhibition and scale morphology by AFM. *J. Colloid Interface Sci.* 240 (2), 608–621.



## Editorial Board of Journal of Environmental Sciences

### Editor-in-Chief

**X. Chris Le** University of Alberta, Canada

### Associate Editors-in-Chief

**Jiuhui Qu** Research Center for Eco-Environmental Sciences, Chinese Academy of Sciences, China  
**Shu Tao** Peking University, China  
**Nigel Bell** Imperial College London, UK  
**Po-Keung Wong** The Chinese University of Hong Kong, Hong Kong, China

### Editorial Board

#### Aquatic environment

**Baoyu Gao**  
Shandong University, China  
**Maohong Fan**  
University of Wyoming, USA  
**Chihpin Huang**  
National Chiao Tung University  
Taiwan, China  
**Ng Wun Jern**  
Nanyang Environment &  
Water Research Institute, Singapore  
**Clark C. K. Liu**  
University of Hawaii at Manoa, USA  
**Hokyong Shon**  
University of Technology, Sydney, Australia  
**Zijian Wang**  
Research Center for Eco-Environmental Sciences,  
Chinese Academy of Sciences, China  
**Zhiwu Wang**  
The Ohio State University, USA  
**Yuxiang Wang**  
Queen's University, Canada  
**Min Yang**  
Research Center for Eco-Environmental Sciences,  
Chinese Academy of Sciences, China  
**Zhifeng Yang**  
Beijing Normal University, China  
**Han-Qing Yu**  
University of Science & Technology of China,  
China

#### Terrestrial environment

**Christopher Anderson**  
Massey University, New Zealand  
**Zucong Cai**  
Nanjing Normal University, China  
**Xinbin Feng**  
Institute of Geochemistry,  
Chinese Academy of Sciences, China  
**Hongqing Hu**  
Huazhong Agricultural University, China  
**Kin-Che Lam**  
The Chinese University of Hong Kong  
Hong Kong, China  
**Erwin Klumpp**  
Research Centre Juelich, Agrosphere Institute  
Germany

#### Peijun Li

Institute of Applied Ecology,  
Chinese Academy of Sciences, China  
**Michael Schloter**  
German Research Center for Environmental Health  
Germany  
**Xuejun Wang**  
Peking University, China  
**Lizhong Zhu**  
Zhejiang University, China

#### Atmospheric environment

**Jianmin Chen**  
Fudan University, China  
**Abdelwahid Mellouki**  
Centre National de la Recherche Scientifique  
France  
**Yujing Mu**  
Research Center for Eco-Environmental Sciences,  
Chinese Academy of Sciences, China  
**Min Shao**  
Peking University, China  
**James Jay Schauer**  
University of Wisconsin-Madison, USA  
**Yuesi Wang**  
Institute of Atmospheric Physics,  
Chinese Academy of Sciences, China  
**Xin Yang**  
University of Cambridge, UK

#### Environmental biology

**Yong Cai**  
Florida International University, USA  
**Henner Hollert**  
RWTH Aachen University, Germany  
**Jaeseong Lee**  
Sungkyunkwan University, South Korea  
**Christopher Rensing**  
University of Copenhagen, Denmark  
**Bojan Sedmak**  
National Institute of Biology, Slovenia  
**Lirong Song**  
Institute of Hydrobiology,  
Chinese Academy of Sciences, China  
**Chunxia Wang**  
National Natural Science Foundation of China  
**Gehong Wei**  
Northwest A & F University, China

#### Daqiang Yin

Tongji University, China  
**Zhongtang Yu**  
The Ohio State University, USA

#### Environmental toxicology and health

**Jingwen Chen**  
Dalian University of Technology, China  
**Jianning Hu**  
Peking University, China  
**Guibin Jiang**  
Research Center for Eco-Environmental Sciences,  
Chinese Academy of Sciences, China  
**Sijin Liu**  
Research Center for Eco-Environmental Sciences,  
Chinese Academy of Sciences, China  
**Tsuyoshi Nakanishi**  
Gifu Pharmaceutical University, Japan  
**Willie Peijnenburg**  
University of Leiden, The Netherlands  
**Bingsheng Zhou**  
Institute of Hydrobiology,  
Chinese Academy of Sciences, China

#### Environmental catalysis and materials

**Hong He**  
Research Center for Eco-Environmental Sciences,  
Chinese Academy of Sciences, China  
**Junhua Li**  
Tsinghua University, China  
**Wenfeng Shangguan**  
Shanghai Jiao Tong University, China  
**Ralph T. Yang**  
University of Michigan, USA

#### Environmental analysis and method

**Zongwei Cai**  
Hong Kong Baptist University,  
Hong Kong, China  
**Jiping Chen**  
Dalian Institute of Chemical Physics,  
Chinese Academy of Sciences, China  
**Minghui Zheng**  
Research Center for Eco-Environmental Sciences,  
Chinese Academy of Sciences, China  
**Municipal solid waste and green chemistry**  
**Pinjing He**  
Tongji University, China

### Editorial office staff

**Managing editor** Qingcai Feng  
**Editors** Zixuan Wang Suqin Liu Kuo Liu Zhengang Mao  
**English editor** Catherine Rice (USA)

# JOURNAL OF ENVIRONMENTAL SCIENCES

环境科学学报(英文版)

[www.jesc.ac.cn](http://www.jesc.ac.cn)

## Aims and scope

*Journal of Environmental Sciences* is an international academic journal supervised by Research Center for Eco-Environmental Sciences, Chinese Academy of Sciences. The journal publishes original, peer-reviewed innovative research and valuable findings in environmental sciences. The types of articles published are research article, critical review, rapid communications, and special issues.

The scope of the journal embraces the treatment processes for natural groundwater, municipal, agricultural and industrial water and wastewaters; physical and chemical methods for limitation of pollutants emission into the atmospheric environment; chemical and biological and phytoremediation of contaminated soil; fate and transport of pollutants in environments; toxicological effects of terrorist chemical release on the natural environment and human health; development of environmental catalysts and materials.

## For subscription to electronic edition

Elsevier is responsible for subscription of the journal. Please subscribe to the journal via <http://www.elsevier.com/locate/jes>.

## For subscription to print edition

China: Please contact the customer service, Science Press, 16 Donghuangchenggen North Street, Beijing 100717, China. Tel: +86-10-64017032; E-mail: [journal@mail.sciencep.com](mailto:journal@mail.sciencep.com), or the local post office throughout China (domestic postcode: 2-580).

Outside China: Please order the journal from the Elsevier Customer Service Department at the Regional Sales Office nearest you.

## Submission declaration

Submission of the work described has not been published previously (except in the form of an abstract or as part of a published lecture or academic thesis), that it is not under consideration for publication elsewhere. The publication should be approved by all authors and tacitly or explicitly by the responsible authorities where the work was carried out. If the manuscript accepted, it will not be published elsewhere in the same form, in English or in any other language, including electronically without the written consent of the copyright-holder.

## Editorial

Authors should submit manuscript online at <http://www.jesc.ac.cn>. In case of queries, please contact editorial office, Tel: +86-10-62920553, E-mail: [jesc@rcees.ac.cn](mailto:jesc@rcees.ac.cn). Instruction to authors is available at <http://www.jesc.ac.cn>.

## Journal of Environmental Sciences (Established in 1989)

Volume 29 2015

<b>Supervised by</b>	Chinese Academy of Sciences	<b>Published by</b>	Science Press, Beijing, China
<b>Sponsored by</b>	Research Center for Eco-Environmental Sciences, Chinese Academy of Sciences		Elsevier Limited, The Netherlands
<b>Edited by</b>	Editorial Office of Journal of Environmental Sciences P. O. Box 2871, Beijing 100085, China Tel: 86-10-62920553; <a href="http://www.jesc.ac.cn">http://www.jesc.ac.cn</a> E-mail: <a href="mailto:jesc@rcees.ac.cn">jesc@rcees.ac.cn</a>	<b>Distributed by</b>	Domestic Science Press, 16 Donghuangchenggen North Street, Beijing 100717, China Local Post Offices through China Foreign Elsevier Limited <a href="http://www.elsevier.com/locate/jes">http://www.elsevier.com/locate/jes</a>
<b>Editor-in-chief</b>	X. Chris Le	<b>Printed by</b>	Beijing Beilin Printing House, 100083, China

CN 11-2629/X

Domestic postcode: 2-580

Domestic price per issue RMB ¥ 110.00

ISSN 1001-0742

